Journal of Hepatocellular Carcinoma

Dovepress
open access to scientific and medical research

Open Access Full Text Article

ORIGINAL RESEARCH

Synergistic Effect of Lenvatinib and Chemotherapy in Hepatocellular Carcinoma Using Preclinical Models

Mingxun Wang[1,*], Xinfei Yao[2,*], Zhiyuan Bo[3,4,*], Jiuyi Zheng[3], Haitao Yu[3], Xiaozai Xie[3], Zixia Lin[3], Yi Wang[5], Gang Chen[3,4], Lijun Wu[3]

[1]Department of Ultrasonography, The First Affiliated Hospital of Wenzhou Medical University, Wenzhou, People's Republic of China; [2]The First Clinical College, Wenzhou Medical University, Wenzhou, People's Republic of China; [3]Department of Hepatobiliary Surgery, The First Affiliated Hospital of Wenzhou Medical University, Wenzhou, People's Republic of China; [4]Key Laboratory of Diagnosis and Treatment of Severe Hepato-Pancreatic Diseases of Zhejiang Province, The First Affiliated Hospital of Wenzhou Medical University, Wenzhou, People's Republic of China; [5]Department of Epidemiology and Biostatistics, School of Public Health and Management, Wenzhou Medical University, Wenzhou, People's Republic of China

*These authors contributed equally to this work

Correspondence: Lijun Wu; Gang Chen, Department of Hepatobiliary Surgery, The First Affiliated Hospital of Wenzhou Medical University, Fuxue Road, Wenzhou, Zhejiang, 325035, People's Republic of China, Tel +86 577 55579-453, Fax +86 577 55579-555, Email wumolijun@163.com; chen.gang@wmu.edu.cn

Purpose: The current study aimed to evaluate the synergistic efficacy of lenvatinib and FOLFOX (infusional fluorouracil (FU), folinic acid, and oxaliplatin) in hepatocellular carcinoma (HCC) using patient-derived xenograft (PDX) and PDX-derived organotypic spheroid (XDOTS) models in vivo and in vitro.

Methods: PDX and matched XDOTS models originating from three patients with HCC were established. All models were divided into four groups and treated with drugs alone or in combination. Tumor growth in the PDX models was measured and recorded, and angiogenesis and phosphorylation of the vascular endothelial growth factor receptor (VEGFR2), rearranged during transfection (RET), and extracellular signal-regulated kinase (ERK) were detected using immunohistochemistry and Western blot assays. The proliferative ability of XDOTS was evaluated through active staining and immunofluorescence staining, and the effect of the combined medication was evaluated using the Celltiter-Glo luminescent cell viability assay.

Results: Three PDX models with genetic characteristics similar to those of the original tumors were successfully established. Combining lenvatinib with FOLFOX led to a higher tumor growth inhibition rate than individual therapies ($P < 0.01$). Immunohistochemical analysis demonstrated that the combined treatment significantly inhibited the proliferation and angiogenesis of PDX tissues ($P < 0.05$), and Western blot analysis showed that the combined treatment significantly inhibited the phosphorylation of VEGFR2, RET, and ERK compared with single-agent treatment. Additionally, all three matched XDOTS models were successfully cultured with satisfactory activity and proliferation, and the combined therapies led to better suppression of XDOTS growth compared with individual therapy ($P < 0.05$).

Conclusion: Lenvatinib combined with FOLFOX had a synergistic antitumor effect in HCC PDX and XDOTS models by inhibiting the phosphorylation of VEGFR, RET, and ERK.

Keywords: hepatocellular carcinoma, lenvatinib, chemotherapy, patient-derived xenografts, angiogenesis

Introduction

Hepatocellular carcinoma (HCC) is a common cancer type worldwide and is prevalent in China owing to viral infections. Although diagnostic technology and therapeutic options have greatly improved, the incidence and mortality of HCC have increased rapidly in recent years.[1] Only one-third of the patients with HCC can benefit from surgical intervention, while others are at a late stage without effective treatment when diagnosed.[2] Currently, molecular targeted therapy and immunotherapy play a crucial role in medical oncology.[3] In recent years, clinical trials assessing immune checkpoint inhibitors (ICIs) in unresectable hepatocellular carcinoma have emerged.[4,5] New molecular targeted drugs, such as

Received: 10 November 2022
Accepted: 11 March 2023
Published: 27 March 2023

lenvatinib[6] in the frontline and regorafenib[7] in the second line, have attracted increasing attention in precision treatment due to their unique antitumor effects in many types of malignant tumors. However, the efficacy of molecular targeted therapy in HCC is not very satisfactory, and the improvement of overall survival by targeted drugs is very limited.[8,9] Lenvatinib is an oral multi-tyrosine kinase inhibitor of vascular endothelial growth factor receptors (VEGFR) 1–3, fibroblast growth factor receptors (FGFR) 1–3, RET, mast/stem cell growth factor receptor kit (SCFR), and oncogenic pathway-related receptor tyrosine kinases (RTKs).[10,11] Combining lenvatinib with other drugs has shown promising efficacy against different cancers.[12–14] Nevertheless, using lenvatinib in combination with other drugs is not satisfactory for patients with unresectable HCC. The FOLFOX regimen (infusional fluorouracil (FU), folinic acid, and oxaliplatin) is the chemotherapy based on the results of an international Phase III clinical study.[15] FOLFOX can serve as a first-line (category 2B) option as recommended by the 2021 National Comprehensive Cancer Network (NCCN) guidelines.[16,17] Both 5-FU and oxaliplatin treatments disrupt DNA replication. However, clinical trials and preclinical studies on lenvatinib combined with the FOLFOX regimen have rarely been reported.

In the past few years, preclinical research has gradually shifted from studying cancer cells to more suitable preclinical models, such as the patient-derived xenograft (PDX) model and three-dimensional (3D) cultured PDX-derived organotypic spheroid (XDOTS) models, especially in the field of oncology.[18–20] A previous study also indicated the possibility of using patient-derived primary cancer cells for drug screening and genomic landscape dissecting.[21] The PDX model, a crucial preclinical model, accurately retains the histopathological and genomic characteristics of the original tumor tissues and provides an ideal model for investigating new therapies and associated mechanisms. However, the low take rate and lengthy implementation time limit the clinical application of PDX. Another limitation of PDX models is that it is challenging to investigate immunotherapeutics in immunodeficient PDX models,[22,23] whereas immunotherapy is a crucial therapy for HCC.[24,25]

This study established PDX and XDOTS models from tumor samples. These two preclinical models, were used to conduct a trial evaluating the efficacy of lenvatinib combined with the FOLFOX regimen in HCC. Furthermore, the current study investigated the associated mechanisms to provide new insights for improving clinical effects in patients with advanced HCC.

Materials and Methods

Establishment of PDX Models

This study was approved by the Ethics Committee of Wenzhou Medical University (ID: WYDW2020-0125) and adhered to the Declaration of Helsinki. All animal experiments complied with the guidelines of the Animal Research Advisory Committee Guidelines. Tumor samples were collected from patients with HCC and informed consent was obtained before surgery. Within 3 h after resection, the samples were aseptically cut into pieces (20–30 mm^3 in size) and then subcutaneously transferred to the front or back of male mice with severe combined immunodeficiency (SCID) for 6–8 weeks (Beijing Vital River Laboratory Animal Technology Co., Ltd., Beijing, China). The mice were housed in an individually ventilated cage system under optimal sanitary conditions, with an average cage temperature of 23°C and relative humidity of 65%. They were fed an autoclaved commercial diet and provided with clean drinking water. Animal husbandry adhered to the triple ethical principles of working with animals, which include reduction, refinement, and replacement. Following the establishment of the first generation of xenografts (F0), serial implant processes were performed in BALB/c nude mice to enlarge the xenograft tumor system (ie, F1, F2, and F3, among others; Figure 1). The tumor volume was calculated as 0.5 × length × $width^2$ using a caliper.

Reagents

Lenvatinib (S1164), oxaliplatin (S1224), 5-FU (S1209), and folinic acid (S1236) were purchased from Selleck Chemicals. 5-FU and oxaliplatin were diluted in 5% dextrose aqueous solution to the final concentrations of 10 mg/mL and 1.2 mg/mL, respectively, and folinic acid was dissolved in a saline solution at a concentration of 3 mg/mL. The study protocols were designed to reflect clinical regimens, and drug doses for mice were calculated using the following formula: mouse dose (mg/kg) = human dose (mg/kg) 37 (hKm) / 3 (mKm), where Km indicates human (h) or mouse (m)

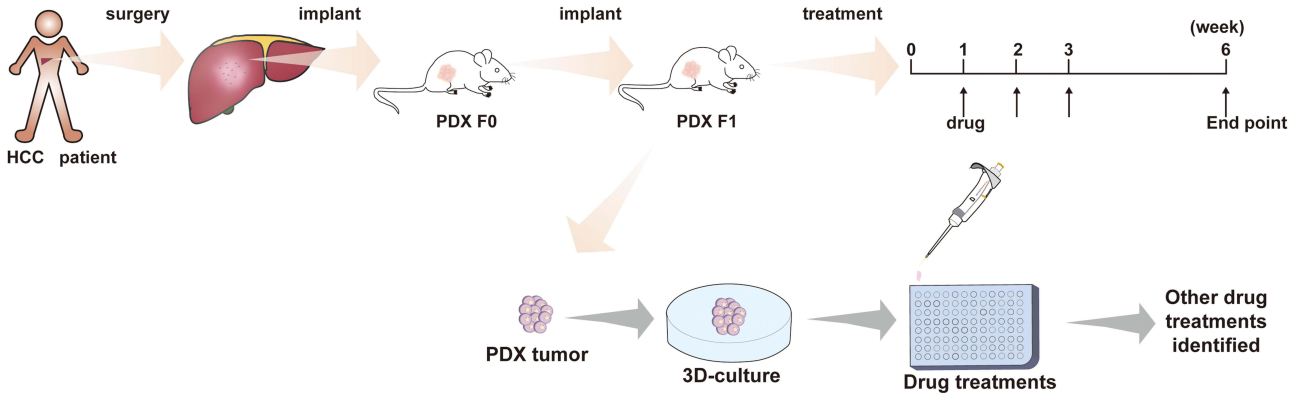

Figure 1 Flowchart of the study program.

body surface coefficient.[26] The order of drug administration was as follows: oxaliplatin (12 mg/kg) was injected intraperitoneally, followed by an intraperitoneal injection of folinic acid (30 mg/kg) 20 min later, and after 40 min, 5-FU (55 mg/kg) was administered. All drugs were administered once a week for six weeks. Moreover, lenvatinib was dissolved in 3 mmol/L diluted hydrochloric acid and administered intragastrically (10 mg/kg) once daily.[27,28]

Short Tandem Repeat (STR) Analysis

To verify that each PDX and XDOTS was derived from the corresponding patient tumor, STR analyses were performed on different chromosomes at 20 loci. Ten nanograms of target DNA were amplified by multiplex polymerase chain reaction (PCR) using fluorescent dye-linked primers for 20 loci:19 autosomal STR loci (D3S1358, D13S317, D7S820, D16S539, Penta E, TPOX, TH01, D2S1338, CSF1PO, Penta D, D19S433, vWA, D21S11, D18S51, D6S1043, D8S1179, D5S818, D12S391, and FGA) and the amelogenin locus on the X chromosome. Amplification was performed using a commercially available EX20 kit from AGCU. The PCR products were processed using an ABI Prism 3130 XL Genetic Analyzer and analyzed using GeneMapper ID v3.2 software (Applied Biosystems).

Effect of Lenvatinib Plus FOLFOX Regimen in PDX Models

When the tumor volume reached approximately 100–200 mm^3, nude mice selected from the F2 generation were randomly divided into four treatment groups (comprising six mice in each group) as follows: (1) vehicle group, (2) lenvatinib group, (3) FOLFOX group, and (4) lenvatinib plus FOLFOX (L+F) group. Additionally, tumor volumes and body weights were monitored three times per week, and the mice were euthanized for further analysis six weeks later.

Establishment of XDOTS Models

XDOTS were cultured as previously described, with slight modifications.[29,30] Briefly, fresh PDX tissues were stored in Roswell Park Memorial Institute medium supplemented with 10% fetal bovine serum (Gemini Bio-Products) and 1% penicillin-streptomycin (Fisher Scientific). PDX tissues were minced into pieces using a sterile scalpel and placed in complete medium containing type IV collagenase (100 U/mL, Life Technologies) and DNase I (50 μg/mL, Roche) for approximately 20 min in a water bath at 37°C. Subsequently, the cell suspension was filtered through a cell strainer (BD Falcon, New Jersey, USA) and centrifuged at 1000 rpm for 5 min. The supernatant was removed, and the pellet was washed with phosphate-buffered saline (PBS) and centrifuged as described above. After mechanical separation by pipetting, the cell pellet was resuspended in an ice-cold 1:1 mixture of the growth medium and Matrigel. Matrigel was polymerized at 37°C for 10 min, and then the growth medium was added to a 24-well plate (500 μL/well).

Cell Viability and Proliferation Assay of XDOTS

The XDOTS models were grown for four days after adding the growth medium to 24-well plates to form compact spheroids. XDOTS models were dissociated by enzymatic dissociation before resuspension in 50 μL of complete

medium (14,000 organotypic spheroids) and plated into 96-well cell-culture plates after coating each well with Matrigel. After 24 h, the supernatant medium was removed, and each well was coated with Matrigel. Subsequently, drugs (5-FU, 10 μg/mL; oxaliplatin, 1 μg/mL; and/or lenvatinib, 10 μM) were administered on day 1, and cultures were maintained up to day 7. Cell proliferation was assessed by CellTiter-Glo (CTG) analysis (Promega, Madison, WI, USA). Additionally, morphological images of the XDOTS models cultured in Matrigel were captured using a phase-contrast confocal microscope (Nikon, Tokyo, Japan). The activity was evaluated using calcein AM (2 μm) and propidium iodide (25 μg/mL) staining. Subsequently, an Olympus Fluoview FV1000 or Zeiss LSM 710 confocal microscope was used for the imaging.

Protein Extraction and Western Blotting

The PDX tissue was transferred to radioimmunoprecipitation assay (RIPA) lysis buffer (Beyotime, P0013B) containing a complete protease inhibitor (Roche, 04693132001), phosSTOP (Roche, 4906837001), and phenylmethylsulfonyl fluoride (PMSF) (Beyotime, ST506). The tissue was minced and homogenized on ice using a polytron homogenizer, and the extracted proteins were analyzed using bicinchoninic acid (BCA) protein assay (Beyotime, P0010). Moreover, proteins were resolved using 10% SDS-PAGE and transferred onto polyvinylidene difluoride membranes (Merck &Millipore, ISEQ00010). After incubation with primary and secondary antibodies, the protein bands were blotted using enhanced chemiluminescence. The antibodies used were as follows: anti-Erk1/2 (1:1000, CST, 4695S), anti-p-ERK1/2(1:1000, AF,1015S), anti-RET (1:1000, CST, 14556S), anti-p-RET (1:1000, CST, 3221S), anti-p-VEGFR2 (1:1000, CST, 3770S), anti-VERGFR2 (1:1000, CST, 2479S), and anti-GAPDH (1:5000, Sigma, G9545).

Histological and Immunohistochemical Analysis

The tissue and XDOTS were fixed in 10% neutral buffered formalin (Sigma) for 24 and 0.5 h, respectively, and then embedded in paraffin. The tissue was cut into 5 μm-thick sections for hematoxylin and eosin (H&E) staining, and the tissue sections were rehydrated with PBS after formalin fixation for immunohistochemical examination. Paraffin slides were deparaffinized, and sodium citrate solution (pH 6.0) was used for antigen retrieval. The slides were incubated in a Tris-Buffered Saline (TBS) solution containing 3% bovine serum albumin (BSA) and 0.5% Triton for 1 h to reduce non-specific background staining and permeabilize the samples. Slides were incubated with the appropriate dilution of the primary antibody at 4°C overnight, and the primary antibodies used were CD31 (1:50; Abcam; ab28364) and Ki-67 (1:200; Abcam; ab16667). Endogenous peroxidase activity was blocked using a 3% hydrogen peroxide/methanol buffer for 15 min. Bound antibodies were detected using the BrightVision Ultimate Kit (Immunology). The slides were washed in TBS and incubated with the secondary antibody-HRP conjugate for 1 h at room temperature, followed by 3,3'-diaminobenzidine (DAB) for 5 min. Finally, the slides were counterstained with hematoxylin and fixed with DPX Mountant for histology (Sigma-Aldrich). Slides were also stained to assess non-specific secondary antibody responses in the absence of the primary antibody. Photographs were taken using a Leica DM 4000 microscope and DFC 450 camera (Leica).

Immunofluorescence Staining of XDOTS

XDOTS samples were rinsed with PBS and fixed in 4% paraformaldehyde for 0.5 h. After fixation, the samples were washed thrice with PBS for 5 min per wash. Subsequently, the samples were permeabilized with 0.3% Triton X-100 for 0.5 h and blocked with 2% BSA in 0.1% Triton X-100 for 30 min. After removing the permeabilization solution, samples were washed again with PBS. Additionally, the samples were treated with the primary antibody— rabbit Anti-Ki67 antibody (1:200; Abcam; ab16667), in 2% BSA overnight at 4°C. The samples were then washed three times with 0.1% Triton X-100 to remove excess antibodies and incubated with goat anti-rabbit secondary antibody (1:200; Abcam; ab150081), phalloidin, and DAPI in 2% BSA for 2 h. Subsequently, the samples were mechanically crushed and released for imaging, and images were captured using a confocal laser-scanning microscope (Nikon A1R).

Statistical Analysis

All experiments were repeated at least three times. The present study used GraphPad Prism Software (version 6.0; San Diego, CA, USA) to perform statistical analyses. All results are presented as mean ± standard deviation (SD). The

differences between groups were analyzed using Student's *t*-test and one-way analysis of variance (ANOVA). Statistical significance was established at a *p*-value <0.05 (*$P < 0.05$; **$P < 0.01$).

Results

Concordance Between Xenografts and Original Tumors

Figure 1 shows that HCC tumor tissues obtained from patients after surgical resection were inoculated into SCID mice for subsequent studies. In a previous study, nine HCC PDX models were successfully established, from which three matched XDOTS models were successfully cultured (Cases 246, 408, and 504). Additionally, STR analysis of DNA isolated from the native tumors and PDX and XDOTS models showed that the native HCC tumors in cases 246, 408, and 504 were compatible with the PDX and XDOTS models, proving that the PDX and XDOTS models could represent the genomic characteristics of the original tumor tissues (Figures 2A and S1). Notably, histological analysis showed that the PDX models retained the differentiated histological features of primary tumor tissues (Figure 2B).

Inhibition Efficacy of Lenvatinib and FOLFOX on PDX Models

The inhibitory effects of lenvatinib combined with FOLFOX therapy in the three HCC PDX models were different. The tumor volumes after different treatments (Figures 3A–C) showed that combining lenvatinib with FOLFOX significantly inhibited tumor growth. Tumor images (Figures 3D–F) and tumor weights (Figures 3G–I) also demonstrated the synergistic inhibitory effect of combination therapy. Interestingly, the present study observed apparent antitumor effects for the three PDX models through combination therapy, which was significant compared to single-agent treatment for the 246 PDX model alone or 246 combined with the 408 PDX model (Figures 3G–J).

Antitumor Effect Associated with Inhibition of Angiogenesis

Immunohistochemical staining demonstrated that the combination therapy of lenvatinib and FOLFOX led to a significant reduction in the expression of Ki-67 and CD31, which are vital signs of angiogenesis and proliferation, indicating that the antitumor activity might be related to the inhibition of tumor angiogenesis and cell proliferation (Figures 4A–C).

Inhibition of Angiogenesis via VEGF/VEGFR/RET/ERK Pathway

The phosphorylation of VEGFR2 and its downstream signaling pathways were examined to clarify the mechanism of the antitumor efficacy of the combination therapy. Western blot analysis showed that VEGFR2, RET, and ERK phosphorylation was significantly inhibited in both the lenvatinib and combination therapy groups (Figures 4D and E). In addition, combining FOLFOX with Lenvatinib demonstrated enhanced effectiveness compared to lenvatinib alone, suggesting that FOLFOX and lenvatinib achieved a synergistic effect.

Spheroid Formation of XDOTS Models

The formation and growth of the 3D XDOTS models were observed, and Figure 5A shows morphological images on days 5, 10, 15, 20, and 25. After seeding on the plate, the cells progressively formed a dense 3D structure, and the size of the structure gradually increased (Figure 5B). Homogeneity between the XDOTS models and native tumors was demonstrated by H&E staining (Figure 5C).

Cell Activity and Proliferation Ability of XDOTS Models

By detecting the expression of Ki-67, it was found that all XDOTS models displayed different proportions of Ki-67+ cells, indicating the proliferative potential of the XDOTS models in vitro (Figures 6A–C). Moreover, calcein AM and propidium iodide staining methods demonstrated the viability of the XDOTS models after the formation of 3D XDOTS models (Figure 6D).

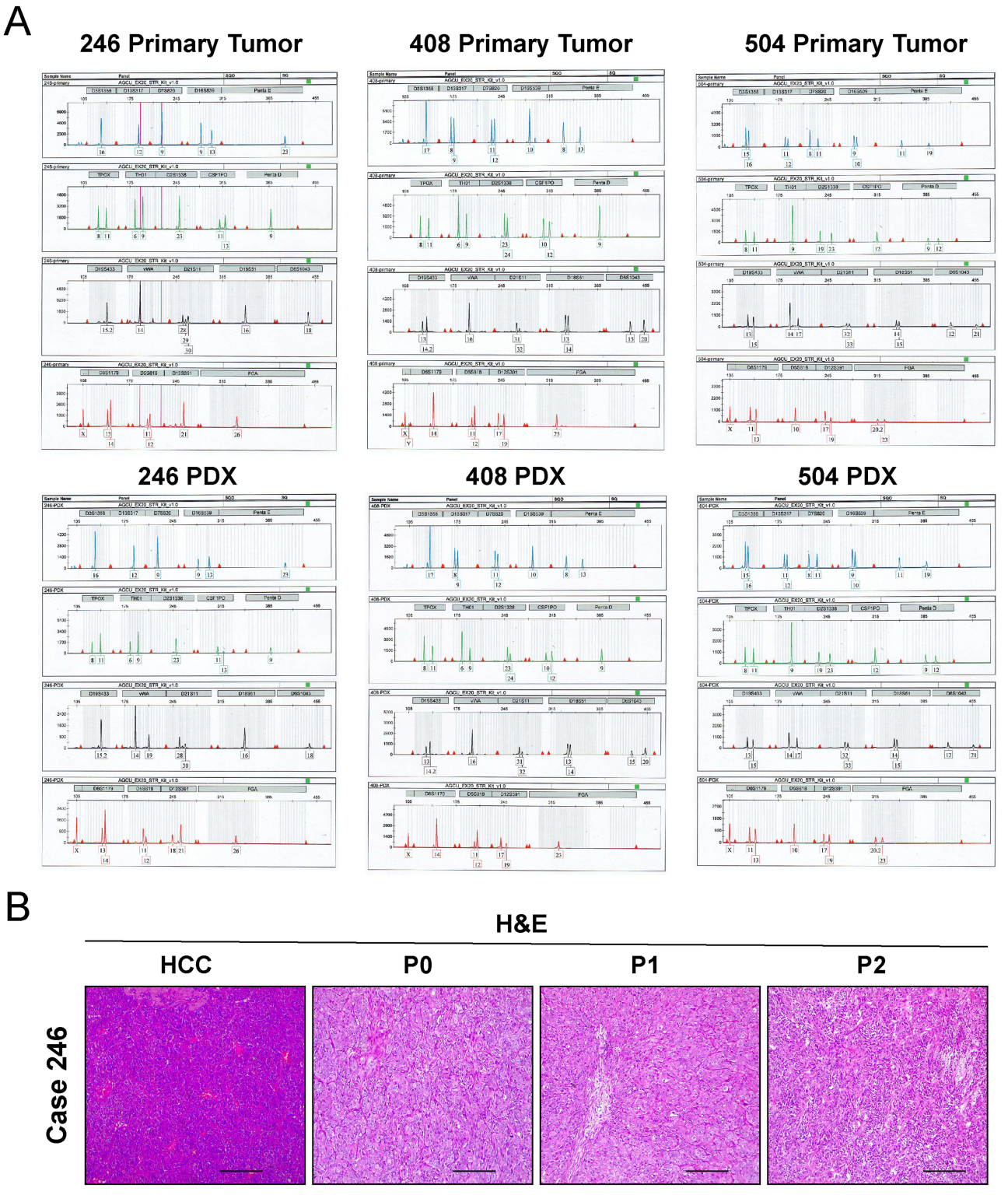

Figure 2 Authentication of PDX models with primary tumors by short tandem repeat analysis. (**A**) STR profiles of primary tumor (Case 246, Case 408 and Case 504) and PDX models (Case 246, Case 408 and Case 504) are shown. (**B**) Representative photomicrographs of H&E staining in case 246. The photomicrographs were captured using the Leica DM 4000 microscope (Leica). Scale bar is 200 μm.

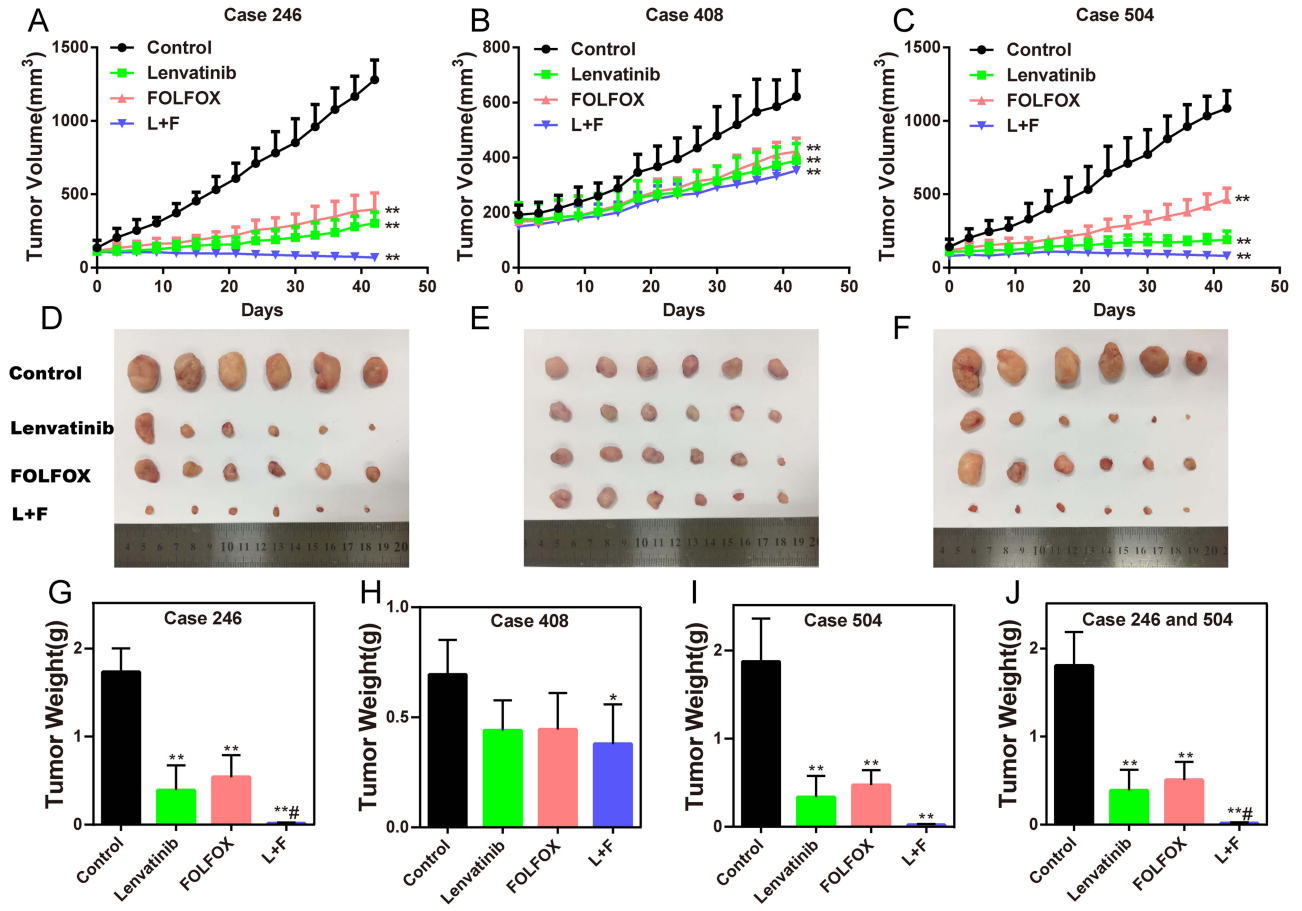

Figure 3 Effect of different drug therapies on PDX models. (**A**–**C**) Growth curves of tumor volumes were recorded for 42 days. The data are expressed as the mean ± SD (n=6 in each group, $^{**}P < 0.01$). (**D**–**F**) Representative images of tumors obtained on day 42 (n=6 in each group). (**G**–**J**) Histogram of tumor weights on day 42. The data are expressed as the mean ± SD (n=6 in each group; $^{*}P < 0.05$, $^{**}P < 0.01$, compared with the control group; $^{\#}P < 0.05$, compared with monotherapy).
Abbreviations: L, lenvatinib; F, FOLFOX.

Inhibition Efficacy of Lenvatinib and FOLFOX on XDOTS Models

The CTG method was used to evaluate the pharmacological effects of lenvatinib and FOLFOX in the XDOTS models. The results suggested that lenvatinib combined with FOLFOX significantly inhibited the activity of the 246 and 504 XDOTS models compared with individual therapies. Additionally, combination therapy significantly inhibited the activity of 408 XDOTS models compared with lenvatinib (Figures 6E–G).

Discussion

Evidently, HCC is a common malignancy and the third leading cause of tumor-related deaths,[31,32] and it is an extremely heterogeneous disease characterized by complex genetic and epigenetic aberrations.[33,34] The present understanding of the HCC heterogeneity and its associated mechanisms is limited, which is a critical obstacle in exploring new treatments for HCC.[35] In this study, the heterogeneity of HCC could be explained by the different findings of the combination therapy observed in the three PDX models, and there was a noticeable synergistic antitumor effect in the three PDX models.

Precision medicine in cancer has recently attracted significant attention, especially in areas of molecularly targeted drugs and ICIs. However, there are still many challenges to be solved in the study of immunotherapy in the immunodeficiency PDX model. Presently, preclinical research is mainly focused on targeted drugs. However, targeted therapy for HCC has not been very successful, and its efficacy remains unsatisfactory. A new targeted drug called lenvatinib has been approved by the American Food and Drug Administration (FDA) for treating HCC.[6] However, the survival benefits remain unsatisfactory in clinical trials. The FOLFOX regimen is another approved first-line treatment option for

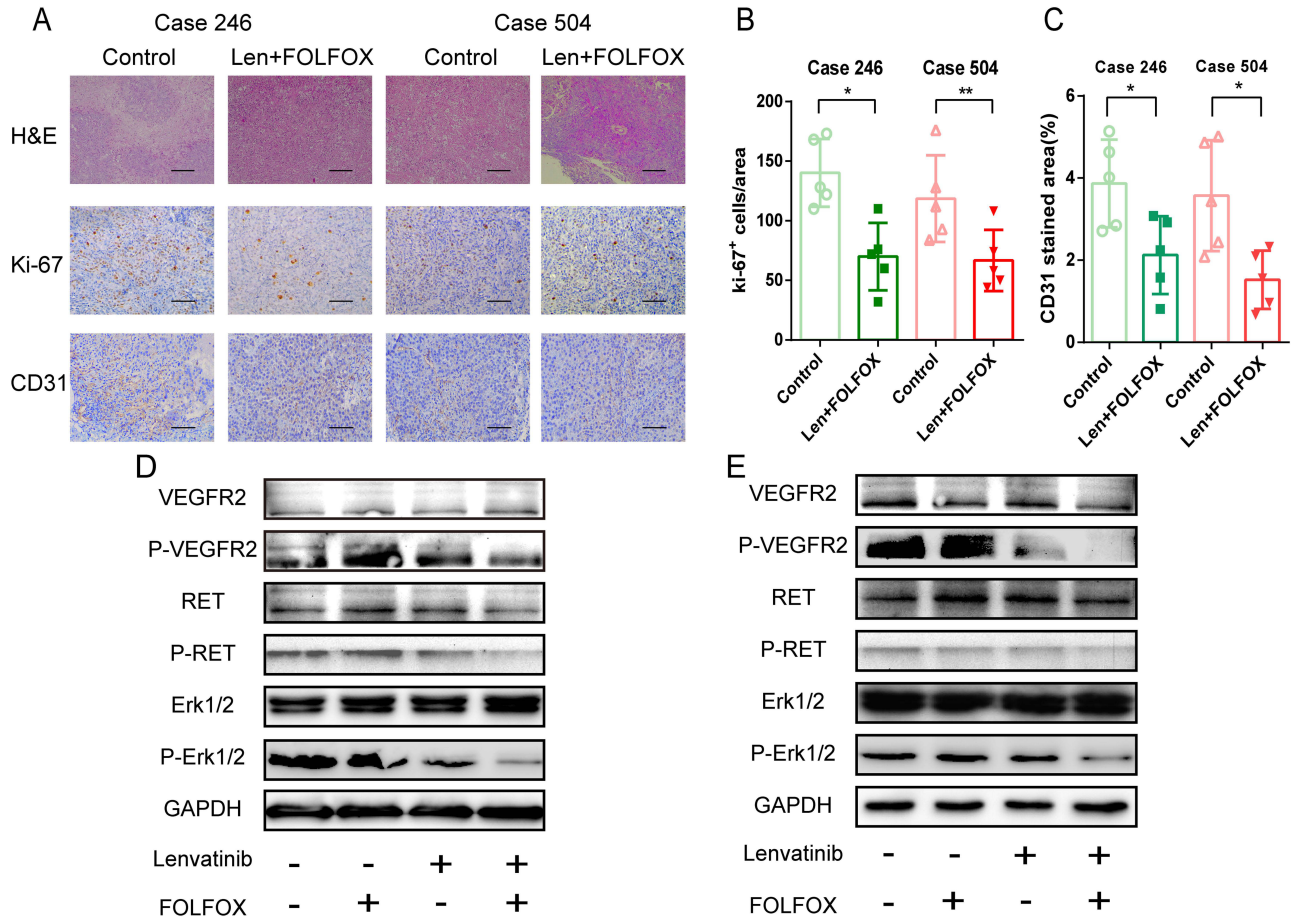

Figure 4 Effect of lenvatinib (10 mg/kg) and FOLFOX (oxaliplatin, 12 mg/kg; 5-FU, 55 mg/kg; folinic acid, 30 mg/kg) on angiogenesis and cell proliferation in PDX models. (**A**) Representative images of H&E, Ki67 and CD31 staining. The photomicrographs were captured using the Leica DM 4000 microscope (Leica). The scale bar is 50 μm. (**B**) Quantification of proliferating cells showing the percentage of Ki-67-positive cells. The data are expressed as the mean ± SD (n=5, *$P < 0.05$, **$P < 0.01$). (**C**) Quantification analysis of tumor-associated endothelial cells showing the number of CD31-positive vascular areas. The data are expressed as the mean ± SD (n=5, *$P < 0.05$). (**D** and **E**) VEGFR2, RET, and ERK levels were measured by Western blotting in 246 PDX and 504 PDX models.
Abbreviation: Len, lenvatinib.

advanced HCC.[16,17] In Phase II clinical trial, FOLFOX combined with sorafenib showed promising results in HCC treatment.[36] Few studies have investigated the use of lenvatinib combined with the FOLFOX regimen for HCC. Based on the different antitumor mechanisms, the present study designed a trial combining lenvatinib and FOLFOX in two preclinical animal models of HCC to assess the efficacy of combination therapy. Ultimately, the present study found that combining lenvatinib with FOLFOX had a more significant inhibitory effect on HCC in vivo and in vitro than monotherapy.

The controversial outcomes between preclinical research and clinical practice are primarily due to a lack of appropriate preclinical tumor models, and the results obtained from preclinical studies cannot accurately represent clinical responses.[37] Traditional preclinical models mainly comprise immortalized cancer cell lines and transgenic mouse models, whose gene expression changes irreversibly.[38] Accumulating phenotypic changes and clonal selection lead to the production of a highly uniform cell population, which cannot perfectly represent the heterogeneity of native tumors.[8] Contrarily, the heterogeneity of native tumors is closely related to tumor development and drug response.[39,40] Therefore, there is an urgent need to establish a reliable preclinical model to examine new drug therapies for HCC.

PDX models have become promising preclinical tools for assessing tumor heterogeneity and drug responses in various malignancies, particularly HCC. It can recapitulate the clinical and biological features of native tumors more accurately than traditional cell line-derived xenografts, and the clinical application of PDX models in drug sensitivity prediction has attracted increasing attention. The current study successfully established several HCC PDX models with

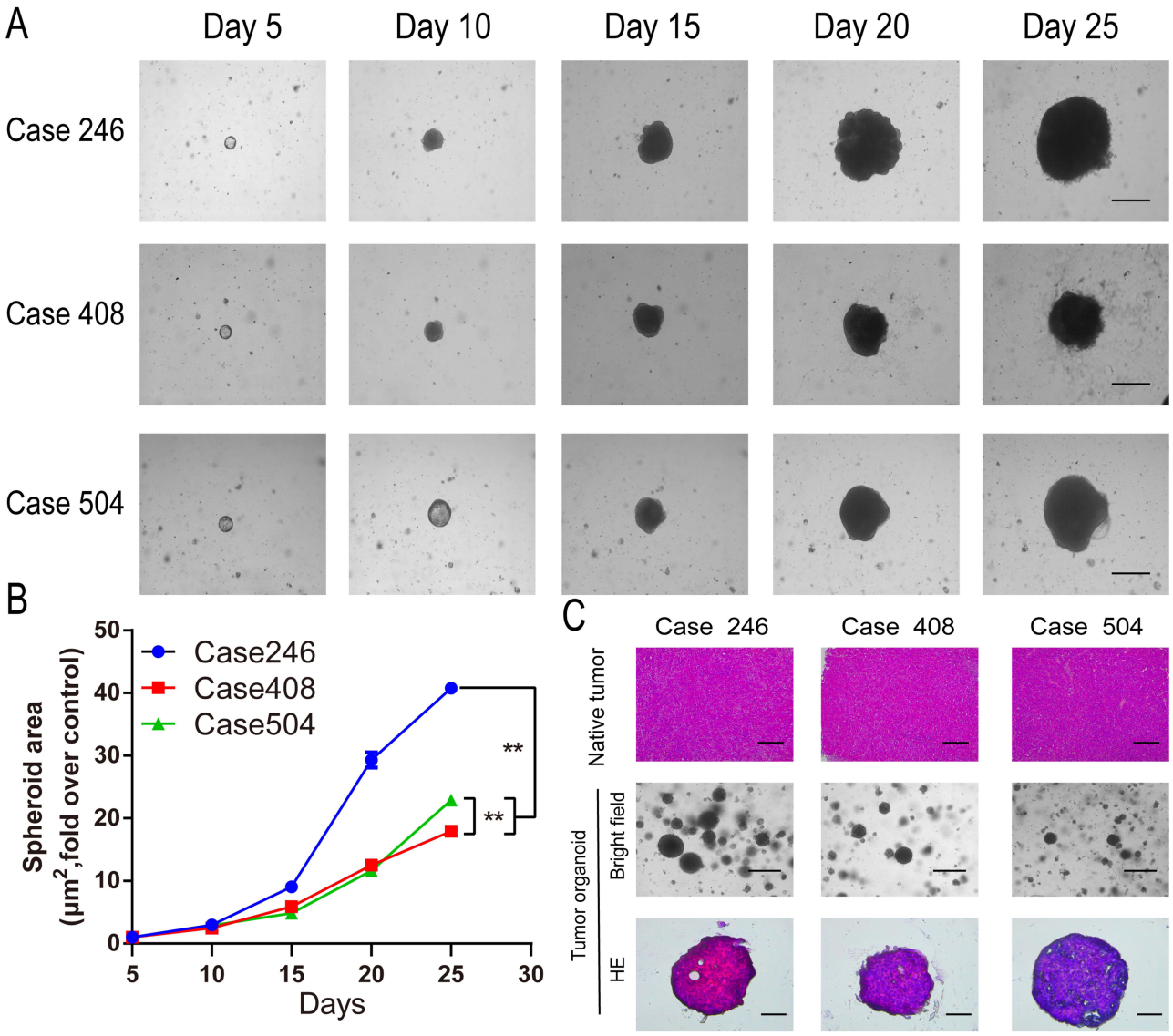

Figure 5 Morphology and growth curves of the XDOTS models. (**A**) Morphology was observed on days 5, 10, 15, 20, and 25. The photomicrographs were captured using a phase-contrast confocal microscope (Nikon). Scale bar is 500 μm. (**B**) Growth curve of XDOTS was recorded for 25 days. The data are expressed as the mean ± SD (n=3, $^{**}P < 0.01$, compared with other groups). (**C**) H&E staining of primary tumors and XDOTS and the morphology of XDOTS were observed. The photomicrographs were captured using the Leica DM 4000 microscope (Leica) and phase-contrast confocal microscope (Nikon). Scale bars represent 200, 20, and 10 μm, respectively.

stable passaging abilities. Using STR analysis, the present study demonstrated that the PDX and XDOTS models have a high degree of consistency with primary tumor tissue, even after several generations.

High cost and low-throughput characteristics limit the application of PDX models in preclinical drug screening. In other studies, the tumor uptake rate of PDX models remains low for HCC (only 20–35%).[41] To overcome these shortcomings, exploring XDOTS models for drug screening has received great attention.[42] The present study established a new 3D cultured XDOTS model based on the relative PDX model in vitro, which is expected to alleviate the high cost and low-throughput limitations of PDX models. In the present study, a range of factors were introduced to the culture medium, namely R-spondin-1, epidermal growth factor (EGF), Noggin Matrigel, nicotinamide, and Y-27632, to stimulate the growth of the XDOTS model. Following a period of 7 days of cultivation, the XDOTS model can be used for drug screening purposes. In contrast, the generation of PDX models is much more time-consuming, taking several months to complete. The present study successfully demonstrated the cell activity and proliferation ability of XDOTS models. Additionally, the drug responses in the XDOTS models were consistent with those in the PDX models in vivo, suggesting

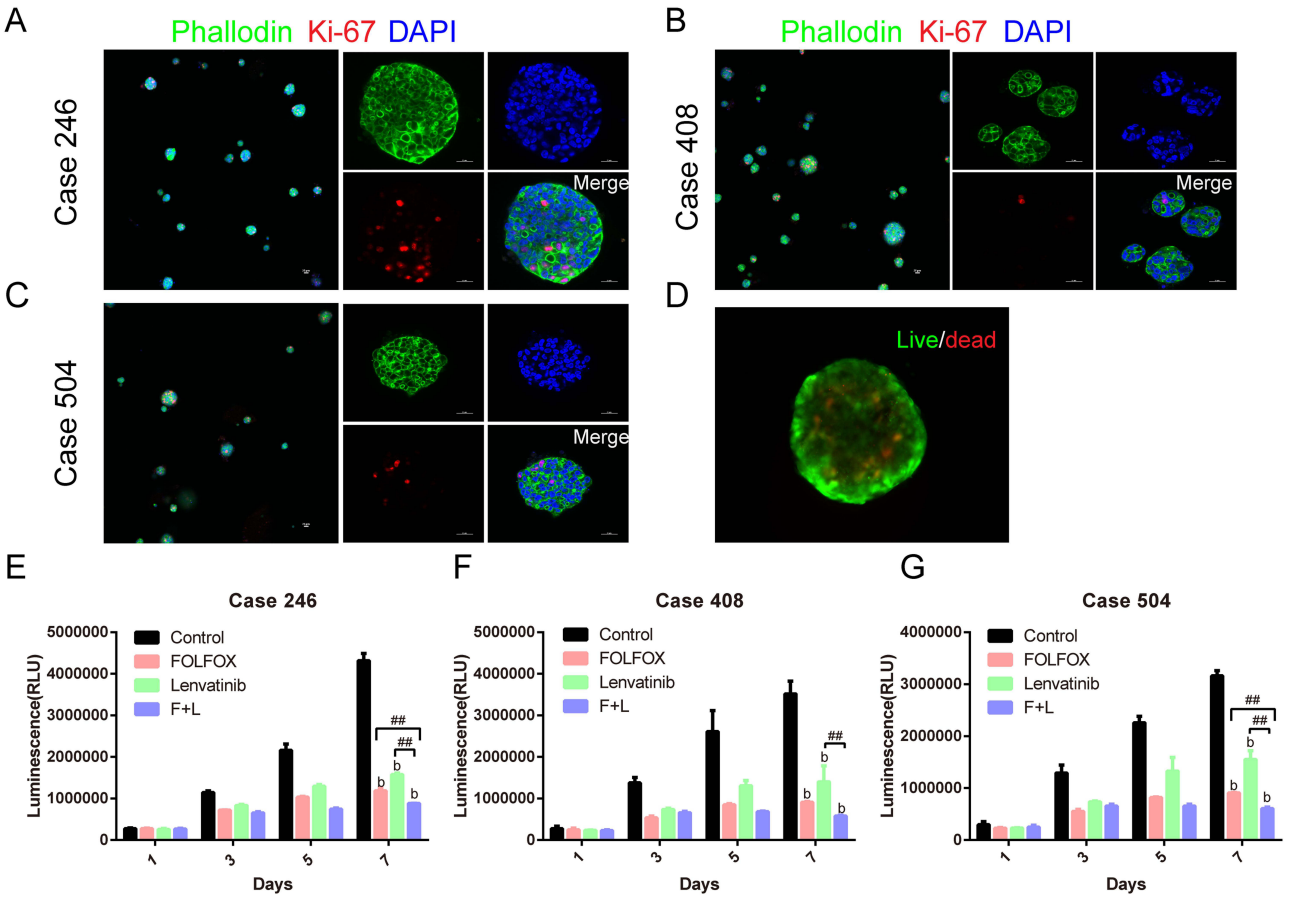

Figure 6 Proliferation ability and drug response in the XDOTS models. (**A**–**C**) Magenta indicates the expression of Ki-67 in proliferating cells. The cells were stained with DAPI (blue) and phalloidin (green) to detect nuclei and actin. Images were captured using a confocal laser-scanning microscope (Nikon A1R). The scale bar is 50 μm. (**D**) Live cells were stained with calcein-AM (green), and dead cells were stained with propidium iodide (red). Images were captured using the Olympus Fluoview FV1000 (Olympus). Scale bar is 100 μm. (**E**–**G**) Inhibitory effects of lenvatinib (10 μM) and FOLFOX (5-FU, 10 μg/mL; oxaliplatin, 1 μg/mL) on XDOTS models after 1 week of drug administration. The data are expressed as the mean ± SD (n=3; b $P < 0.01$, compared to the control group; $^{\#\#}P < 0.01$, compared with monotherapy).
Abbreviations: L, lenvatinib; F, FOLFOX.

that the XDOTS models might partly replace some PDX experiments. This might be a promising preclinical model and may play an important role in translational research in the future.

HCC development is a complex process that involves cell proliferation, invasion, migration, and angiogenesis. Angiogenesis has been shown to significantly influence the survival and proliferation of HCC cells. CD31 is an essential indicator of angiogenesis, whereas Ki67 is an important indicator of proliferation. The current study assessed the potential mechanisms underlying the synergistic antitumor efficacy of lenvatinib and FOLFOX combination therapy for HCC. Finally, the present study concluded that the expression of Ki67 and CD31 in the tissue was significantly reduced after combination therapy, suggesting that the antitumor activity may depend on the effective inhibition of tumor angiogenesis and cell proliferation. The present study further investigated the signaling pathways involved in the anti-angiogenic effects. Based on the results obtained in this study, we were able to demonstrate that combining lenvatinib and FOLFOX effectively inhibits VEGF within the VEGFR2 / RET / RET / ERK signaling pathway.

There are some limitations to the current study. First, the tumor take rate for the PDX and XDOTS models is not very high and stable, which might be due to the heterogeneity of tumor tissues and individual microenvironments. Some studies have reported that mixing tissues with Matrigel plus growth factors can enhance the uptake rate in the PDX model.[43] Moreover, because of the limited sample size of the animal models used in the current study, the findings need to be further validated in large-scale experiments.

Conclusion

The current study showed that lenvatinib combined with FOLFOX had a synergistic antitumor effect in PDX and XDOTS models by inhibiting the phosphorylation of VEGFR, RET, and ERK. In addition, establishing PDX and XDOTS model platforms can provide new insights for preclinical research on novel therapies.

Abbreviations

FOLFOX, folinic acid fluorouracil oxaliplatin; HCC, Hepatocellular carcinoma; PDX, patient-derived xenograft; XDOTS, PDX-derived organotypic spheroids; FDA, Food and Drug Administration; 3D, three-dimensional; SCID, severe combined immunodeficiency; STR, Short tandem repeat; PCR, polymerase chain reaction; PBS, phosphate-buffered saline; CTG, CellTiter-Glo; RIPA, radioimmunoprecipitation assay; BCA, bicinchoninic acid; BSA, bovine serum albumin; DAB, diaminobenzidine; SD, standard deviation; ANOVA, one-way analysis of variance; EGF, epidermal growth factor; VEGFR, vascular endothelial growth factor receptor; RET, Rearranged during Transfection; ERK, extracellular signal regulated kinase; TBS, tris-buffered saline; H&E, hematoxylin and eosin; ICIs, immune checkpoint inhibitors; NCCN, National Comprehensive Cancer Network.

Ethical Standards

This trial was approved by the Ethics Committee of Wenzhou Medical University (ID: WYDW2020-0125) and adhered to the Declaration of Helsinki. All animal experiments complied with the National Research Council's Guide for the Care and Use of Laboratory Animals.

Acknowledgments

This work was supported by the Research Foundation of National Health Commission of China- Major Medical and Health Technology Project for Zhejiang Province grant number WKJ-ZJ-1706. This work was also supported by the 2021 National Innovation Project of College Students in China (202110343019) and the 2020 Science and Technology Innovation Activity Plan for Students in Zhejiang Province (2020R413022). This work was also supported by the Wenzhou Major Scientific and Technological Innovation Key Medical and Health Project (ZY2022006).

Disclosure

The authors declare no competing interests related to this work.

References

1. Siegel R, Miller K, Fuchs H, Jemal A. Cancer statistics, 2022. *CA*. 2022;72(1):7–33. doi:10.3322/caac.21708
2. Chung AS, Mettlen M, Ganguly D, et al. Immune checkpoint inhibition is safe and effective for liver cancer prevention in a mouse model of hepatocellular carcinoma. *Cancer Prev Res*. 2020;13(11):911–922. doi:10.1158/1940-6207.CAPR-20-0200
3. Rizzo A, Ricci AD, Di Federico A, et al. Predictive biomarkers for checkpoint inhibitor-based immunotherapy in hepatocellular carcinoma: where do we stand? *Front Oncol*. 2021;11. doi:10.3389/fonc.2021.803133
4. Di Federico A, Rizzo A, Carloni R, et al. Atezolizumab-bevacizumab plus Y-90 TARE for the treatment of hepatocellular carcinoma: preclinical rationale and ongoing clinical trials. *Expert Opin Investig Drugs*. 2022;31(4):361–369. doi:10.1080/13543784.2022.2009455
5. Rizzo A, Ricci A, Gadaleta-Caldarola G, Brandi G. First-line immune checkpoint inhibitor-based combinations in unresectable hepatocellular carcinoma: current management and future challenges. *Expert Rev Gastroenterol Hepatol*. 2021;15(11):1245–1251. doi:10.1080/17474124.2021.1973431
6. Kudo M, Finn RS, Qin S, et al. Lenvatinib versus sorafenib in first-line treatment of patients with unresectable hepatocellular carcinoma: a randomised Phase 3 non-inferiority trial. *Lancet*. 2018;391(10126):1163–1173. doi:10.1016/s0140-6736(18)30207-1
7. Rizzo A, Nannini M, Novelli M, Dalia Ricci A, Scioscio VD, Pantaleo MA. Dose reduction and discontinuation of standard-dose regorafenib associated with adverse drug events in cancer patients: a systematic review and meta-analysis. *Ther Adv Med Oncol*. 2020;12:175883592093693. doi:10.1177/1758835920936932
8. Gao Q, Wang Z-C, Duan M, et al. Cell culture system for analysis of genetic heterogeneity within hepatocellular carcinomas and response to pharmacologic agents. *Gastroenterology*. 2017;152:1. doi:10.1053/j.gastro.2016.09.008
9. Levatić J, Salvadores M, Fuster-Tormo F, Supek F. Mutational signatures are markers of drug sensitivity of cancer cells. *Nat Commun*. 2022;13(1):2926. doi:10.1038/s41467-022-30582-3
10. Tohyama O, Matsui J, Kodama K, et al. Antitumor activity of lenvatinib (e7080): an angiogenesis inhibitor that targets multiple receptor tyrosine kinases in preclinical human thyroid cancer models. *J Thyroid Res*. 2014;2014:638747. doi:10.1155/2014/638747
11. Okamoto K, Ikemori-Kawada M, Jestel A, et al. Distinct binding mode of multikinase inhibitor lenvatinib revealed by biochemical characterization. *ACS Med Chem Lett*. 2015;6(1):89–94. doi:10.1021/ml500394m

12. Makker V, Taylor MH, Aghajanian C, et al. Lenvatinib plus pembrolizumab in patients with advanced endometrial cancer. *J Clin Oncol*. 2020;38(26):2981–2992. doi:10.1200/JCO.19.02627
13. Taylor MH, Lee C-H, Makker V, et al. Phase IB/II trial of lenvatinib plus pembrolizumab in patients with advanced renal cell carcinoma, endometrial cancer, and other selected advanced solid tumors. *J Clin Oncol*. 2020;38(11):1154–1163. doi:10.1200/JCO.19.01598
14. Kawazoe A, Fukuoka S, Nakamura Y, et al. Lenvatinib plus pembrolizumab in patients with advanced gastric cancer in the first-line or second-line setting (EPOC1706): an open-label, single-arm, Phase 2 trial. *Lancet Oncol*. 2020;21(8):1057–1065. doi:10.1016/S1470-2045(20)30271-0
15. Qin S, Bai Y, Lim HY, et al. Randomized, multicenter, open-label study of oxaliplatin plus fluorouracil/leucovorin versus doxorubicin as palliative chemotherapy in patients with advanced hepatocellular carcinoma from Asia. *J Clin Oncol*. 2013;31(28):3501–3508. doi:10.1200/JCO.2012.44.5643
16. Hou Z, Liu J, Jin Z, et al. Use of chemotherapy to treat hepatocellular carcinoma. *Biosci Trends*. 2022;16(1):31–45. doi:10.5582/bst.2022.01044
17. Benson A, D'Angelica M, Abbott D, et al. Hepatobiliary cancers, version 2.2021, NCCN clinical practice guidelines in oncology. *JNCCN*. 2021;19(5):541–565. doi:10.6004/jnccn.2021.0022
18. Hidalgo M, Amant F, Biankin AV, et al. Patient-derived xenograft models: an emerging platform for translational cancer research. *Cancer Discov*. 2014;4(9):998–1013. doi:10.1158/2159-8290.CD-14-0001
19. Abdolahi S, Ghazvinian Z, Muhammadnejad S, Saleh M, Asadzadeh Aghdaei H, Baghaei K. Patient-derived xenograft (PDX) models, applications and challenges in cancer research. *J Transl Med*. 2022;20(1):206. doi:10.1186/s12967-022-03405-8
20. Han S, Wu J. Three-dimensional (3D) scaffolds as powerful weapons for tumor immunot herapy. *Bioact Mater*. 2022;17:300–319. doi:10.1016/j.bioactmat.2022.01.020
21. Crystal AS, Shaw AT, Sequist LV, et al. Patient-derived models of acquired resistance can identify effective drug combinations for cancer. *Science*. 2014;346(6216):1480–1486. doi:10.1126/science.1254721
22. Byrne AT, Alférez DG, Amant F, et al. Interrogating open issues in cancer precision medicine with patient-derived xenografts. *Nat Rev Cancer*. 2017;17(4):254–268. doi:10.1038/nrc.2016.140
23. Zanella ER, Grassi E, Trusolino L. Towards precision oncology with patient-derived xenografts. *Nature Rev*. 2022;19(11):719–732. doi:10.1038/s41571-022-00682-6
24. Mohammed A, Shoemaker RH, Sei S. Cancer immunoprevention: challenges and potential opportunities for use of immune checkpoint inhibitors. *Cancer Prev Res*. 2020;13(11):897–900. doi:10.1158/1940-6207.CAPR-20-0432
25. Llovet J, Castet F, Heikenwalder M, et al. Immunotherapies for hepatocellular carcinoma. *Nat Rev Clin Oncol*. 2022;19(3):151–172. doi:10.1038/s41571-021-00573-2
26. Reagan-Shaw S, Nihal M, Ahmad N. Dose translation from animal to human studies revisited. *FASEB J*. 2007;22(3):659–661. doi:10.1096/fj.07-9574LSF
27. Mattei F, Kato Y, Tabata K, et al. Lenvatinib plus anti-PD-1 antibody combination treatment activates CD8+ T cells through reduction of tumor-associated macrophage and activation of the interferon pathway. *PLoS One*. 2019;14(2):e0212513. doi:10.1371/journal.pone.0212513
28. Nakagawa T, Matsushima T, Kawano S, et al. Lenvatinib in combination with golvatinib overcomes hepatocyte growth factor pathway-induced resistance to vascular endothelial growth factor receptor inhibitor. *Cancer Sci*. 2014;105(6):723–730. doi:10.1111/cas.12409
29. Ivanova E, Kuraguchi M, Xu M, et al. Use of patient-derived tumor organotypic spheroids to identify combination therapies for mutant non-small cell lung cancer. *Clin Cancer Res*. 2020;26(10):2393–2403. doi:10.1158/1078-0432.CCR-19-1844
30. Yu M, Selvaraj SK, Liang-Chu MMY, et al. A resource for cell line authentication, annotation and quality control. *Nature*. 2015;520(7547):307–311. doi:10.1038/nature14397
31. Bray F, Ferlay J, Soerjomataram I, Siegel RL, Torre LA, Jemal A. Global cancer statistics 2018: GLOBOCAN estimates of incidence and mortality worldwide for 36 cancers in 185 countries. *CA Cancer J Clin*. 2018;68(6):394–424. doi:10.3322/caac.21492
32. Sperandio R, Pestana R, Miyamura B, Kaseb A. Hepatocellular carcinoma immunotherapy. *Annu Rev Med*. 2022;73:267–278. doi:10.1146/annurev-med-042220-021121
33. Hou Y, Guo H, Cao C, et al. Single-cell triple omics sequencing reveals genetic, epigenetic, and transcriptomic heterogeneity in hepatocellular carcinomas. *Cell Res*. 2016;26(3):304–319. doi:10.1038/cr.2016.23
34. Yang F, Hilakivi-Clarke L, Shaha A, et al. Metabolic reprogramming and its clinical implication for liver cancer. *Hepatology*. 2023. doi:10.1097/hep.0000000000000005
35. Zheng H, Pomyen Y, Hernandez MO, et al. Single-cell analysis reveals cancer stem cell heterogeneity in hepatocellular carcinoma. *Hepatology*. 2018;68(1):127–140. doi:10.1002/hep.29778
36. Goyal L, Zheng H, Abrams TA, et al. A phase II and biomarker study of sorafenib combined with modified FOLFOX in patients with advanced hepatocellular carcinoma. *Clin Cancer Res*. 2019;25(1):80–89. doi:10.1158/1078-0432.CCR-18-0847
37. Honkala A, Malhotra SV, Kummar S, Junttila MR. Harnessing the predictive power of preclinical models for oncology drug development. *Nat Rev Drug Discov*. 2021. doi:10.1038/s41573-021-00301-6
38. McGranahan N, Swanton C. Clonal heterogeneity and tumor evolution: past, present, and the future. *Cell*. 2017;168(4):613–628. doi:10.1016/j.cell.2017.01.018
39. Chaisaingmongkol J, Budhu A, Dang H, et al. Common molecular subtypes among asian hepatocellular carcinoma and cholangiocarcinoma. *Cancer Cell*. 2017;32:1. doi:10.1016/j.ccell.2017.05.009
40. Ma L, Heinrich S, Wang L, et al. Multiregional single-cell dissection of tumor and immune cells reveals stable lock-and-key features in liver cancer. *Nat Commun*. 2022;13(1):7533. doi:10.1038/s41467-022-35291-5
41. Xin H, Wang K, Hu G, et al. Establishment and characterization of 7 novel hepatocellular carcinoma cell lines from patient-derived tumor xenografts. *PLoS One*. 2014;9(1):e85308. doi:10.1371/journal.pone.0085308
42. Kim J, Koo B-K, Knoblich JA. Human organoids: model systems for human biology and medicine. *Nat Rev Mol Cell Biol*. 2020;21(10):571–584. doi:10.1038/s41580-020-0259-3
43. Hu B, Li H, Guo W, et al. Establishment of a hepatocellular carcinoma patient-derived xenograft platform and its application in biomarker identification. *Int J Cancer*. 2020;146(6):1606–1617. doi:10.1002/ijc.32564